An experimental investigation of two module configurations for use in active segmented partitions

Timothy W. Leishman

Acoustics Research Group, Department of Physics and Astronomy, Brigham Young University, Eyring Science Center, Provo, Utah 84602

Jiri Tichy

Graduate Program in Acoustics, The Pennsylvania State University, Applied Science Building, University Park, Pennsylvania 16802

Individual modules intended for active segmented partitions should be carefully analyzed before they are advanced as viable tools for active sound transmission control. In this paper we present experimental evaluations of two vibration-controlled modules: a single-composite-leaf (SCL) configuration and a double-composite-leaf (DCL) configuration. Experimental apparatuses and procedures are introduced to assess their normal-incidence transmission losses over a bandwidth from 40 to 1970 Hz. The average transmission loss of the passive SCL module is found to be 21 dB. If its transmitting diaphragm acceleration is minimized through active control, transmission loss increases somewhat at lower frequencies but decreases at higher frequencies, producing no increase in the average value. The average transmission loss of the passive DCL module is found to be 43 dB. After its transmitting diaphragm acceleration is actively minimized, the transmission loss increases substantially at all frequencies (especially at low frequencies), to produce an average value of 77 dB. Thus, while both configurations have the same underlying control objective, the DCL module yields a 56 dB average improvement over the SCL module through simple configurational changes. An alternative control scheme is investigated that minimizes acoustic pressure in the DCL module cavity, but it is found to be less effective. © 2005 Acoustical Society of America. [DOI: 10.1121/1.1992747]

I. INTRODUCTION

An active segmented partition (ASP) consists of an array of interconnected modules or elements with active and passive components that are configured and controlled to reduce sound transmission. Proper design, control, and evaluation of individual modules are crucial if ASPs are to provide effective control of sound transmission over useful bandwidths. In the past, research of ASPs has been obscured by more extensive research in other areas of active sound transmission control (ASTC).[1] It has nevertheless been pursued by a few researchers, who have seen its potential to enhance sound isolation capabilities of existing segmented partition structures, reduce partition masses, simplify active control requirements, and enhance ASTC in other ways.

Acousticians have long recognized the need for more efficient control of sound transmission through lightweight partitions, particularly at low frequencies. Some have anticipated that the active control of partitions would help fulfill this need because of its typical low-frequency benefits. However, difficulties encountered in the control of distributed structural and fluid media have imposed serious limitations on both the performance and practicality of many ASTC systems. Several criteria have been proposed to address these limitations, suggesting that properly implemented ASPs could provide needed ASTC improvements.[2,3]

Most researchers advocating ASPs in the past have done so to propose a means of controlling sound transmission through fuselage structures into aircraft cabins.[4–10] This concept is appealing because interior fuselage trim panels already exist as segmented partition elements. Others have suggested ASPs to control sound transmission through lightweight machinery enclosure walls[11,12] (a concept reminiscent of earlier passive techniques[13]). The authors of this paper have explored many different ASP configurations for general applications and ASTC improvements.[2,3,14–17]

While past research efforts have provided useful contributions to ASPs and their advancement, they have often lacked in-depth analyses and comparisons of module configurations, control methods, and associated ASTC performances. Recent theoretical work has filled some of these gaps through the exploration of several distinct module configurations.[2,3,17] However, a presentation of related experimental results is needed to validate theoretical predictions, to further compare the configurations, and to establish those capable of producing very high transmission loss using simple control strategies.

Sound isolation capabilities of experimental ASP implementations have often remained ambiguous to readers of the literature. Apparent shortcomings related to their performance and consistency have limited their acceptance or utility for many applications. However, uncertainty surrounding their capabilities has arisen in part because irregular measurement techniques are often used to quantify sound isolation of active partitions. While it is true that their measure-

ments are somewhat unique and must account for special conditions produced by active control,[18] they should reasonably conform to recognized norms, providing a meaningful evaluation of actual transmission loss capabilities. Experimental methods have been developed as part of this work to address these needs.

The research reported in this paper was undertaken to increase general understanding of ASPs and to provide greater insight into individual module configurations, their performance capabilities, and their limitations. It was also intended to substantiate theoretical predictions for two specific ASP module configurations. The first incorporated a single electromechanically actuated diaphragm with a surrounding airtight suspension (compare configuration 2 in Ref. 17). Theoretical work predicted that this single-composite-leaf (SCL) configuration would show significant transmission loss deficiencies. The second involved an electroacoustic actuator driving an isolated cavity and thereby actuating a passive transmitting diaphragm with a surrounding airtight suspension (compare configuration 3 in Ref. 17). Theoretical work predicted that this double-composite-leaf (DCL) configuration would perform much better than the first, achieving very high transmission loss over a broad bandwidth while satisfying several other design and performance criteria.[2,3,17]

Several experimental tools were developed to evaluate the modules and their control schemes. The underlying control objective for each was to minimize sound transmission through global reduction of transmitting surface vibrations, using only simple actuation and error-sensing techniques.

In the following sections we describe the experimental methods used in the research effort. We then present results and analyses of measured normal-incidence transmission losses for the two modules in their passive and active states. The results are compared to theoretical predictions and transmission losses of six passive benchmark partitions for further experimental validation and insight.

II. EXPERIMENTAL METHODS

A. Transmission loss measurement system

Normal-incidence acoustic properties of ASP modules may be readily determined using plane-wave tubes and the two-microphone transfer function technique developed by Chung and Blaser.[20,21] The common uses of these tools for the measurement of absorptive materials and acoustic filters naturally extend to the measurement of an electromechanoacoustic device separating a source tube and receiving tube.[3,14,15,22] The approach may be used to decompose the upstream and downstream fields adjacent to an ASP module into normally incident, reflected, and transmitted components, producing reliable transmission loss measurements. The possible residual reflection from an anechoic receiving tube termination suggests a need to decompose the downstream field into traveling-wave components using downstream microphones.

Figure 1 depicts the plane-wave tube system developed for the measurement of ASP modules and passive benchmark partitions in this work. It is shown with an arbitrary partition
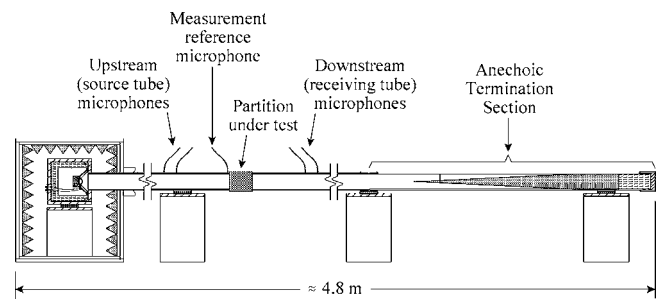

FIG. 1. Experimental system for measuring normal-incidence transmission loss of an individual partition module (ASP module or passive benchmark structure). The arrangement is shown with an arbitrary partition positioned between the source tube and receiving tube.

positioned between the source tube and receiving tube. Time-averaged sound power incident upon a partition $\langle W_i \rangle_t$ and transmitted through the partition $\langle W_t \rangle_t$ are detected using the upstream and downstream microphone pairs. The transmission loss then follows from the expression

$$\text{TL} = 10 \log \left(\frac{\langle W_i \rangle_t}{\langle W_t \rangle_t} \right). \tag{1}$$

Both tubes were constructed of heavy plastic with 10.1 cm inside diameters.[23] The source tube had an overall length of approximately 1 m. The receiving tube consisted of a measurement section and an anechoic termination section. The termination was designed following empirical concepts[24] and validated[25] using the two-microphone transfer function technique.[26] It was a pyramidal wedge cut from a block of 25.6 kg/m³ open-cell polyurethane foam rubber, tapering over a 91 cm span from its apex to its 10.1 cm diameter circular base. Its tip was supported by a thin wire set a small distance from the apex to prevent it from sagging. The circular base was a 25 cm thick continuous extension of the wedge, backed by an 18 cm thick air cavity filled with loose glass-wool insulation and capped with a heavy cast-iron plug. In overall length, the anechoic termination was approximately 134 cm. Its measured cutoff frequency (above which its normal-incidence pressure-amplitude reflection coefficient modulus was consistently $|R| \leq 0.10$) was approximately 135 Hz. However, its absorption coefficient α exceeded 0.5 down to 40 Hz. The usable length of the receiving tube measurement section, from a given partition face to the anechoic wedge tip, was approximately 184 cm.

The source tube excitation loudspeaker was driven by an amplified swept sinusoid, stepped at 1 Hz increments below the cutoff frequency of the first tube cross mode (1990 Hz). Many partitions introduced boundary conditions that resulted in significant axial source tube resonances. However, acoustic pressure was measured by a measurement reference microphone at the source-side face of each partition to ensure that its level was maintained at a nearly constant value over frequency. This was accomplished through automatic level control of the excitation signal. The process ensured sufficiently linear behavior of the source tube sound field and its transducers, and maintained an adequate transmission loss signal-to-noise ratio at all frequencies of interest. Nevertheless, because of the automatic control, the excitation loud-
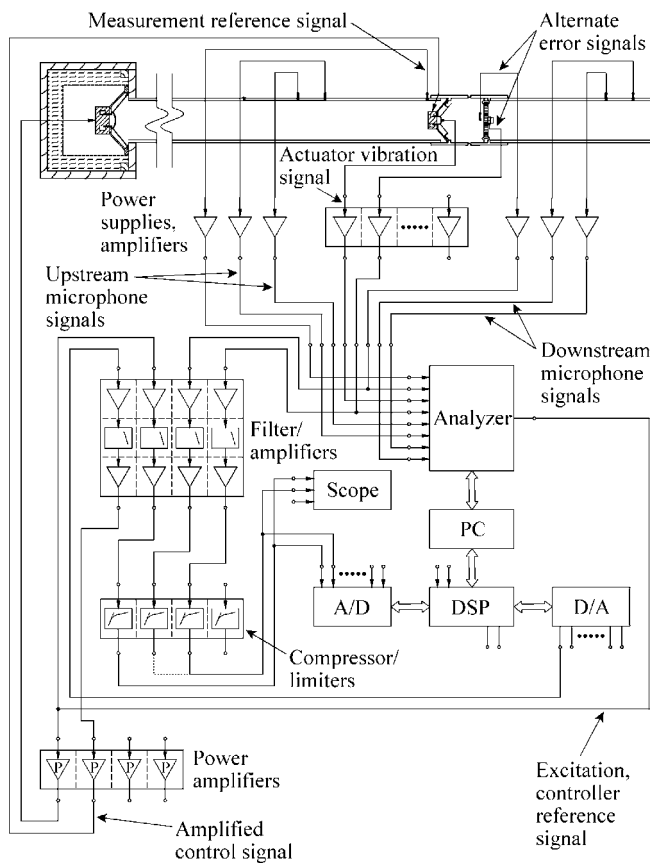
FIG. 2. Block diagram showing electronic equipment and interconnections of the measurement system. The interconnections shown correspond to the evaluation of the double-composite-leaf (DCL) ASP module discussed in Sec. III B.


FIG. 3. Single-composite-leaf (SCL) ASP module, shown with an accelerometer mounted to the transmitting diaphragm (aluminum honeycomb sandwich disk). Compare configuration 2 of Ref. 17.

speaker vibrated more vigorously at some frequencies (i.e., at source tube antiresonance frequencies) than at other frequencies (i.e., at source tube resonance frequencies). Structure-borne flanking transmission consequently became more conspicuous near antiresonance frequencies.

A block diagram of the measurement system, its transducers, and electronics is shown in Fig. 2. Rough placements of microphones and accelerometers are suggested in the figure. More specific placements are discussed below and shown in subsequent figures. Holes were drilled into the tops of the source and receiving tubes to accept microphones at key positions and multiple spacings. This enabled broadband decomposition of the fields within established error constraints.[26,27] The microphones were regularly calibrated to each other and to a standard reference microphone using switching[20,26] and uniform-pressure calibration techniques.

As seen from the figure, three microphones were actually used to probe the source tube. The microphone positioned closest to the partition (approximately 1 cm upstream) was the measurement reference microphone mentioned earlier. The other two microphones were a relatively calibrated pair used to determine the one-dimensional acoustic properties in the source tube. The rightmost microphone of the pair was fixed 30 cm (approximately 3 tube diameters) from the end of the tube. This distance provided a margin beyond the common single-diameter rule,[26] allowing a greater decay of strongly reflected higher-order modes and ensuring the plane

wave mode became more predominant at the microphone pair. The leftmost microphone of the pair was positioned at one of two upstream positions to provide either a 7.0 or 42.0 cm microphone spacing for valid measurements at higher or lower frequencies, respectively. A second relatively calibrated microphone pair was used in a mirror-image configuration on the opposite side of the partition to probe the receiving tube. A usable measurement bandwidth of approximately 40 to 1970 Hz was made possible through the combination of measurements made with the two spacings. A few passive properties of ASP modules were evaluated at frequencies below 40 Hz. Error conditions did not fall into the ideal range for these frequencies,[27] but they were considered reasonable for the purposes of this study. Other details of the measurement system, control system, and electronics are discussed in Ref. 3.

B. ASP modules

1. Single-composite-leaf (SCL) module

The first experimental ASP module was adapted from a moving-coil loudspeaker, as shown in Fig. 3. The loudspeaker diaphragm was replaced by an aluminum honeycomb sandwich disk with a 7 cm diameter and an 11 g total mass. Because its first bending mode frequency (for a free-edge condition) was determined to be well above the cutoff frequency of the first plane-wave tube cross mode, the disk was assumed to behave as a rigid body over the frequency range of interest. A small 1.3 g acrylic tube was glued between the existing voice-coil former and disk to enable its direct electromechanical actuation. The inner edge of the existing half-roll doped-cloth surround was glued to the back face of the disk around its periphery. The loudspeaker frame incorporated large openings, making it somewhat unobtrusive to incident waves.

The loudspeaker mounting flange was trimmed to fit snugly within a heavy PVC plastic tube coupler and firmly adhered to the inner coupler surfaces to produce an airtight seal between the source tube and receiving tube. The coupler was likewise joined to the source tube and receiving tube with airtight seals. An accelerometer was mounted to the center of the transmitting face of the disk as an error sensor. When the module was excited by normally incident waves, a control signal could be applied to the actuator terminals to
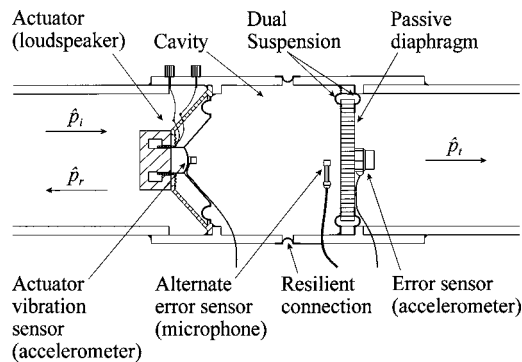
FIG. 4. Double-composite-leaf (DCL) ASP module, shown with accelerometers mounted to the hardened actuator diaphragm dust dome and to the passive transmitting diaphragm. A cavity microphone is also shown behind the center of the transmitting diaphragm. The module coupler housings are attached via a resilient airtight connection to reduce structure-borne flanking transmission from the source tube to the receiving tube. Compare configuration 3 of Ref. 17.

minimize the normal acceleration of the disk. In its uncontrolled state, the actuator terminals were simply open circuited. Electro-mechano-acoustic parameters for the module (defined in Ref. 17) were determined using common electric impedance testing techniques,[28] acoustical testing techniques,[22] direct measurements,[3] and published specifications.

2. Double-composite-leaf (DCL) module

The second experimental ASP module is depicted in Fig. 4. It was constructed using the same type of loudspeaker as in the first module, but with the original diaphragm assembly still intact. The diaphragm dust dome was coated with several layers of epoxy to provide a sufficiently rigid surface for accelerometer mounting. A miniature accelerometer was mounted to the dome to observe its vibrational behavior. In this configuration, the loudspeaker functioned as an electroacoustic actuator driving a small acoustic cavity (11.3 cm diameter and 9.1 cm nominal length) between its own diaphragm and a passive transmitting diaphragm. The latter consisted of a 19 g stiff aluminum honeycomb sandwich disk supported by a dual surrounding suspension. The suspension consisted of two half-roll butyl 50 rubber surrounds that were firmly glued to the peripheries of the front and back disk faces. An accelerometer was mounted to the center of the transmitting face as an error sensor. A small microphone was also positioned in the cavity to observe the enclosed field or to act as an alternate error sensor. Electro-mechano-acoustic parameters for the module (defined in Ref. 17) were again determined using a variety of methods.

As with the first module, the actuator and transmitting diaphragm assemblies were carefully fitted and adhered within tube coupler housings with airtight seals. The couplers were also joined to the source tube and receiving tube with airtight seals. However, because of complications arising from flanking transmission during very high transmission loss measurements, the two couplers were typically spaced by about 1 cm and joined with a resilient airtight connection. The connection reduced structure-borne flanking trans-

mission into the receiving tube, most of which resulted from mechanical source tube vibrations induced by the excitation loudspeaker or control actuator.

Once the module was excited by normally incident waves, a control signal was applied to the actuator terminals to minimize either normal acceleration of the transmitting diaphragm or acoustic pressure at a specified point within the cavity. In its uncontrolled state, the actuator terminals were open-circuited.

C. Passive benchmark partitions

As a means of validating results provided by the measurement system, the active and passive transmission losses of the experimental ASP modules were compared with transmission losses of several passive benchmark partitions. Table I summarizes the designs and experimental purposes of the various active and passive structures.

Benchmark partition 1 was an open tube (no structure), expected to provide very little if any measurable transmission loss. Benchmark partition 2 was the isolated passive transmitting diaphragm assembly from the DCL ASP module. The transmission loss of this diaphragm was expected to behave like that of a single-leaf partition with effective mass, compliance, and resistance over an appreciable bandwidth.

Benchmark partition 3 incorporated a single 2.5 cm thick, 11.3 cm diameter solid steel plug spanning the entire cross section of a PVC plastic or steel tube coupler, sealed around its periphery to the inner surfaces of the coupler. The coupler was firmly connected and sealed to both the source and receiving tube. While the structure had no readily predictable transmission loss behavior, it was expected to provide a high transmission loss benchmark with significant structural flanking paths. Benchmark partition 4 (also shown in Fig. 5) incorporated a pair of sealed steel plugs—one in a PVC coupler and one in an adjacent steel coupler. As with the DCL ASP module, one coupler was mounted and sealed to the source tube and the other was mounted and sealed to the receiving tube. They were typically separated from each other by a 1 cm spacing and joined with a resilient airtight connection. This resulted in a plug spacing of approximately 4 cm. The arrangement provided a very high transmission loss benchmark. The resilient connection could also be removed so that the couplers could be firmly connected or separated by a large distance (e.g., 50 cm). Additional physical separation further reduced direct and flanking transmission, providing an extremely high transmission loss, near or exceeding the highest measurable transmission loss of the experimental system.

Benchmark partition 5 was an arrangement similar in basic form to the SCL ASP module (see Fig. 3). However, the transmitting diaphragm, surround, voice-coil assembly, and spider were removed from the actuator and replaced with a heavy steel plug (see Fig. 6). The diameter of the plug face was the same as the diameter of the transmitting aluminum honeycomb sandwich disk. The diameter of the plug shaft was approximately the same as the diameter of the voice-coil former and extension. The base of the shaft was firmly affixed to the actuator magnet structure. Since the resilient sur-

TABLE I. Listing of measured ASP modules and passive benchmark partitions.

Name	Description	Purpose	Diagram
SCL ASP module	Single-composite-leaf ASP module	TL evaluation of configuration 2 from Ref. 17.	
DCL ASP module	Double-composite-leaf ASP module, resilient coupler connection	TL evaluation of configuration 3 from Ref. 17.	
Benchmark partition 1	Open tube	Validation of minimal TL	
Benchmark partition 2	Single-leaf passive transmitting diaphragm	Validation of predictable single-leaf partition TL	
Benchmark partition 3	Single steel plug	High TL with appreciable structure-borne flanking	
Benchmark partition 4	Dual steel plugs, resilient coupler connection	Very high TL with minimal structure-borne flanking	
Benchmark partition 5	Modified SCL module, steel plug, no surround	TL evaluation of magnet and diaphragm constriction	
Benchmark partition 6	Modified SCL module, steel plug, surround	TL evaluation of isolated surround	
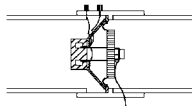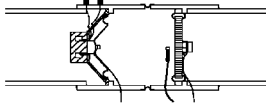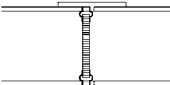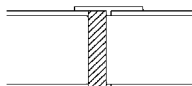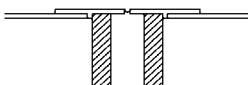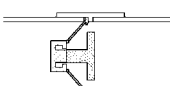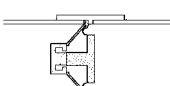
round was removed, a direct but constricted sound transmission path was introduced around the perimeter of the plug.

Benchmark partition 6 was nearly identical to benchmark partition 5, except that the resilient surround was once again mounted. As shown in Fig. 6, its inner edge was glued to the steel plug and its outer edge was glued to the actuator frame. This mounting again established the airtight seal between the source and receiving tubes and provided an approximate passive means of evaluating sound transmission through the surround alone.

D. Measurement capabilities and limitations

Measurements and analyses of the first four passive benchmark partitions were conducted to verify that the mea-

surement system functioned as expected and to identify some of its capabilities and limitations. The open tube (benchmark partition 1) showed little if any transmission loss (never exceeding 0.4 dB) over the measurement bandwidth. The isolated passive transmitting diaphragm assembly (benchmark partition 2) closely followed its theoretically predicted behavior as a single-leaf partition. The single and dual steel plug partitions (benchmark partitions 3 and 4) demonstrated the high transmission loss measurement capabilities of the system, but also exposed certain limitations. Maximum reliable transmission loss values were limited by flanking transmission, electronic cross-talk, ambient acoustic noise, electronic noise, etc. Benchmark partition 3 yielded a
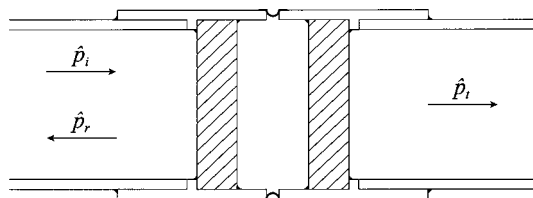
FIG. 5. Passive benchmark partition 4: a pair of spaced 2.5 cm thick solid steel plugs spanning the entire cross sections of the tube couplers to which they are sealed. The couplers are shown as being attached to each other by a resilient airtight connection to reduce structure-borne flanking transmission from the source tube to the receiving tube.
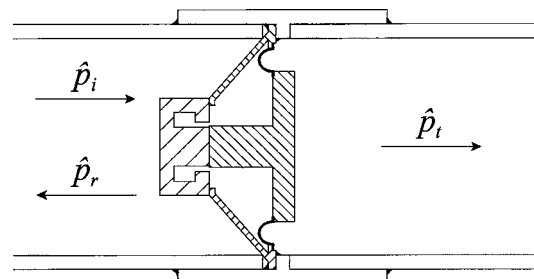
FIG. 6. Passive benchmark partition 6: a modified SCL module with a steel plug replacing the transmitting diaphragm assembly. The surround is intact.
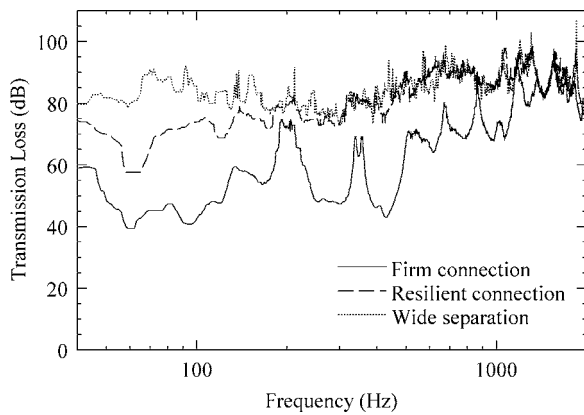
FIG. 7. Measured transmission losses for passive benchmark partition 4 (see Fig. 5). Measurement results are shown for three distinct coupler interconnection conditions.

transmission loss ranging from approximately 50 dB at the lowest measurement frequencies to approximately 70 dB at the highest frequencies, with an average value of 60 dB.[29] However, the transmission loss curve had several significant undulations over frequency that corresponded to decreases and increases in structural flanking transmission near the axial source tube resonance and antiresonance frequencies, respectively (see Sec. II A).

Many of the same flanking transmission effects were evident (especially below 700 Hz) for the dual steel plug partition (benchmark partition 4) when the couplers were rigidly connected. When the couplers were spaced with the resilient connection between them, these effects largely disappeared below 1350 Hz and the measurable transmission loss dramatically increased. The value ranged from approximately 70 dB at the lowest frequencies to approximately 90 dB above 500 Hz, with an average transmission loss of 86 dB. If the resilient connection was removed and the couplers were widely separated with no mechanical connection at all, a significant increase in the measured transmission loss occurred at only the lowest frequencies, below about 160 Hz. In this case, the transmission loss ranged from approximately 80 dB at the lowest frequencies to approximately 90 dB at the highest frequencies, producing only a slightly higher average value. Transmission loss plots for the three coupler conditions are shown in Fig. 7.

The benchmark partitions also increased the understanding of the experimental ASP modules. As discussed in Sec. III A 2, measurements of benchmark partitions 5 and 6 were particularly useful for increasing understanding of the SCL module. Other validations of the measured module properties are discussed in Ref. 3.

The transmission loss curves in Fig. 7 demonstrate a degree of random fluctuation at decibel values above about 80 dB. In such a high decibel range, measurement limitations could be caused by electronic cross-talk between measured signals or an insufficient electroacoustic signal-to-noise ratio. A series of measurements specifically demonstrated that electronic cross-talk could impact the associated downstream signals—at least near 200 Hz, 350 Hz, and in the band between 500 and 1000 Hz.[3] Electroacoustic noise in the downstream measurements included ambient noise and self-noise

of the microphones and their accompanying electronics. Because of the signal processing methods used in the measurements, the upstream incident intensity level was intended to exceed the transmission loss by an amount greater than the associated background intensity level at all frequencies of interest. For partitions with extremely high transmission loss, this could pose a significant problem. The incident intensity level had to be limited to prevent clipping of source-space microphone signals and other system nonlinearities. A level of approximately 124 dB (re 10^{-12} W/m^2) was chosen, producing a maximum transmission loss signal-to-noise ratio from roughly 80 dB at the lowest frequencies to 100 dB at the highest frequencies. The average value over the measurement bandwidth was approximately 95 dB.[3]

A comparison of the measured transmission loss of benchmark partition 4 (with resilient connection) to the maximum measurable values (limited by either electronic crosstalk or transmission loss signal-to-noise ratio) revealed that the partition pushed the dynamic limits of the measurement system—especially between 500 and 800 Hz. However, at most other frequencies, the system was capable of measuring its average 86 dB transmission loss with sufficient margin. Other measurement limitations and sources of measurement error are considered elsewhere.[3,22,26,27]

E. Measurement challenges posed by adaptive control

Additional experimental challenges needed to be surmounted to perform accurate transmission loss measurements of the ASP modules under adaptive control. Simultaneous (and sometimes conflicting) dynamic range requirements dictated by the measurement system and the adaptive controller had to be consistently satisfied. The adaptive controller also had to remain stable and maintain an adequate rate of convergence as it tracked the swept-sinusoidal stimulus.

1. Simultaneous dynamic range requirements

As seen in Fig. 2, several components of the measurement system shared signals with the adaptive controller. The challenging simultaneous dynamic range requirements of the components became further complicated by the fact that the measurement system utilized multiple signal channels and a large bandwidth. To maximize usable dynamic ranges, it was necessary to optimize signal path gain structures. The analyzer automatically adjusted every A/D input range with internal amplification circuits; they were checked, adjusted, and recorded with each swept-sine step. However, the adaptive controller had no automatic gain control for its A/D inputs. The associated signals had to be independently conditioned and optimized to ensure that the controller dynamic range capabilities could be met.

As indicated above, the ambient acoustic and electronic noise present in the receiving tube measurements required the source tube to be sufficiently but not excessively driven to bring transmitted acoustic energy above the noise floor. This was a primary reason why the stimulus signal level was adjusted over frequency to maintain a nearly constant sound pressure level at the source-side face of the partitions. The

process necessitated frequency-dependent compensation for the excitation loudspeaker sensitivity and strong source tube resonances. However, the same signal driving the excitation loudspeaker power amplifier also drove the adaptive controller reference input. Thus, because of the extreme amplitude adjustments needed to satisfy the constant sound pressure level requirement, the varying signal level essentially pushed the adaptive controller input to its dynamic limits. Had the signal at the input been maintained at a consistent optimal level, the dynamic range of transmission loss measurements would have suffered. Thus, the ideal requirements of the measurement system and adaptive controller were essentially at odds with one another.

The solution chosen to remedy this problem involved both the use of the measurement reference microphone discussed earlier and the multichannel dbx 1046 compressor/limiter, which conditioned the controller reference input signal (see Fig. 2). The latter was set with an infinite compression ratio and a threshold that maintained a nearly constant controller reference input level over the entire measurement bandwidth. Another channel of the compressor/limiter was used to explore dynamic range control of the ASP module error signals.[30]

Because of the automatic stimulus signal level adjustments, the excitation loudspeaker required protection from being overdriven at some frequencies. This was accomplished by specifying a fixed maximum stimulus signal level in the swept-sine control. The output signal of the reference microphone was also maintained at a maximum level that ensured that the sound pressure at all other source-space microphones would remain high, but without overdriving them or their accompanying electronic circuitry.

2. Tracking of the swept-sine stimulus

Another experimental challenge involved the ability of the adaptive controller to track rapid changes in the stepped-sinusoidal excitation of the measurement system. With measurements spanning nearly 2000 Hz with 1 Hz step intervals, overall measurement durations could be quite long. It was therefore desirable to adjust the sweep rate to be as fast as possible and the settling time after each step to be as short as possible. However, the adaptive controller had to be able to track the sweep, adapting rapidly and stably within the settling times.

As the stimulus frequency approached axial source tube resonance frequencies, the adaptive controller typically took much longer to adapt after each 1 Hz frequency increment. This was likely due to dramatic changes in system amplitudes and phases near these frequencies. On occasion, it was necessary to increase settling times or pause measurements and increase adaptive controller convergence parameters to shorten convergence times with each step.

III. RESULTS

The experimental ASP modules were tested under the various conditions summarized in Table II. Three measure-

TABLE II. Measurement conditions for the experimental ASP modules.

ASP Module	Mode	Error Signal	Error Signal Compression
SCL	Passive	N/A	N/A
	Active	Transmitting diaphragm acceleration	No
		Transmitting diaphragm acceleration	Yes
DCL	Passive	N/A	N/A
	Active	Transmitting diaphragm acceleration	Yes
		Cavity pressure, behind diaphragm center	Yes
		Cavity pressure, behind diaphragm periphery	Yes

ments were conducted for the SCL module and four for the DCL module. The following sections provide additional details of these measurements and their results.

A. Single-composite-leaf (SCL) module

The SCL module depicted in Fig. 3 was evaluated under two basic conditions. First, its behavior was measured in its passive mode, with the actuator terminals open circuited. Subsequently, its normal transmitting diaphragm acceleration was minimized through adaptive control. The acceleration control was first achieved without error signal compression, then with error signal compression. The following paragraphs report measurements and observations for the module under the various conditions. They also compare evaluations of passive benchmark partitions 5 and 6 introduced in Sec. II C.

1. Passive mode

Figure 8 shows the measured normal-incidence transmission loss for the passive module plotted against the transmission loss for the active module (discussed below). Passive and active theoretical predictions are also plotted using analytical results[17] and module parameters. The minimum
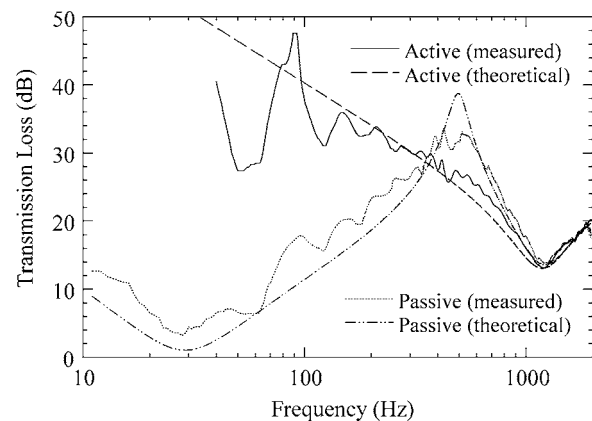

FIG. 8. Measured transmission losses for the SCL ASP module in its passive mode (actuator terminals open circuited) and in its active mode (transmitting diaphragm acceleration minimized). The measured curves are plotted against theoretical predictions for the two modes.

value of the passive transmission loss curve corresponds to the diaphragm assembly resonance frequency at approximately 28 Hz. Below this frequency, the assembly becomes stiffness controlled. Between about 50 and 500 Hz, it appears to behave as a mass-controlled single-leaf partition; its value consistently rises at approximately 6 dB per octave.[31] One might expect the device to remain mass controlled at higher frequencies, but this behavior clearly breaks down above 500 Hz. The transmission loss drops from a maximum of 32 dB at 500 Hz to 14 dB at about 1220 Hz. It then rises again gradually, but to a value no greater than 20 dB. The dip centered at 1220 Hz corresponds to the primary resonance of the damped surround. When averaged over the entire measurement bandwidth, the transmission loss of the passive module is approximately 21 dB.

2. Transmitting diaphragm acceleration control

The normal acceleration of the module diaphragm was effectively minimized through direct electromechanical actuation. As indicated earlier, this actuation could be adaptively controlled either with or without compression of the acceleration error signal. Despite improvements in error signal reduction provided by compression,[32] transmission losses produced by the module were essentially identical in either case.

The actively controlled transmission loss shown in Fig. 8 generally agrees with the corresponding theoretical prediction, except at the lowest frequencies. The measured curve decreases with undulation from moderate values (e.g., 35 dB) at low frequencies to a minimum value of 13 dB at 1220 Hz. The curve then rises by approximately 1 dB per 100 Hz increase to a value of about 20 dB at 1970 Hz. The average transmission loss over the entire measurement bandwidth is again 21 dB. Thus, on average, the actively controlled module offers no benefit over the passively controlled module. However, below 350 Hz, it does offer useful improvement. Between 40 and 350 Hz, the average transmission loss is 33 dB, compared to the 24 dB average of the uncontrolled module. At the lowest frequencies, active control produced a 20 to 30 dB improvement over the passive transmission loss results.

As predicted theoretically, the uncontrolled module provided better transmission loss than the controlled module between about 350 and 1300 Hz. Above 1300 Hz, the controlled and uncontrolled states produced essentially identical results. Theoretical analysis suggested that these high-frequency active performance limitations are caused by uncontrolled surround vibrations.[17] Passive benchmark partitions 5 and 6 were evaluated to validate this assertion. Benchmark partition 5 provided means of evaluating the constriction effects of the module magnet structure, frame, and rigid transmitting diaphragm core. Benchmark partition 6 was identical to benchmark partition 5, except that it added the flexible airtight surround (see Fig. 6). Measured transmission losses of the two benchmark partitions are compared in Fig. 9.

Without the surround, the transmission loss of benchmark partition 5 was very small. Over the measurement bandwidth, its average value was only 1 dB. It produced a
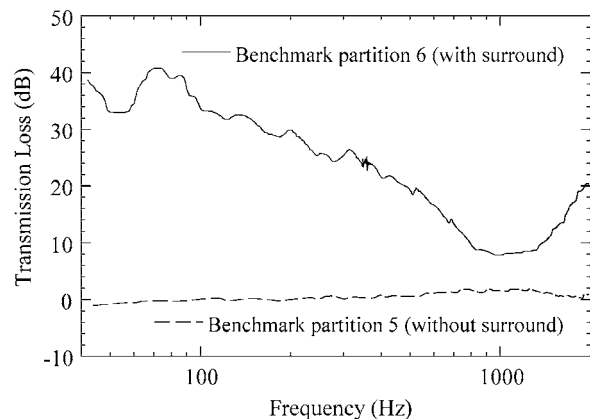

FIG. 9. Measured transmission losses for passive benchmark partitions 5 and 6 (see Fig. 6). Both are modified SCL modules with a steel plug replacing the transmitting diaphragm assembly. Benchmark partition 5 is configured without a surround while benchmark partition 6 is configured with a surround.

transmission loss plateau of just under 2 dB between 750 and 1275 Hz. At higher and lower frequencies, the transmission loss tapered to values closer to those of the open tube, with an average transmission loss of less than 0.2 dB. The transmission loss of benchmark partition 6 was quite similar to that of the acceleration-controlled ASP module shown in Fig. 8. These measurements accordingly confirm that the module surround was an important partition element with a resonant transmission loss minimum near 1200 Hz.

B. Double-composite-leaf (DCL) module

The DCL module depicted in Fig. 4 was evaluated under three basic conditions. It was first measured in its passive mode, with its actuator terminals open circuited. It was next measured in its first active mode, with its normal transmitting diaphragm acceleration minimized through acoustic actuation. It was subsequently measured in its second active mode, with its enclosed cavity pressure minimized at a point through acoustic actuation. For the second active mode, the error signal was first produced by a microphone located on the chamber axis, centered about 1 cm behind the transmitting diaphragm. The microphone was then moved to a position about 1 cm from the edge of the chamber, approximately 1 cm behind the transmitting diaphragm surround. Because of the success of error signal compression with the SCL module, the compressor/limiter was again used to process the module error signals (see Fig. 2). In the following sections we provide evaluations of the module under the various conditions.

1. Passive mode

The measured normal-incidence transmission loss for the passive DCL module is shown in Fig. 10. A theoretical curve based on analytical results[17] and module parameters is also shown for comparison. The dip in the curve to its minimum value near 35 Hz is well predicted by the theoretical curve and is caused by the impedances of the actuator and transmitting diaphragm assemblies. Transmission loss is characteristically poor in the surrounding spectral region. Al-
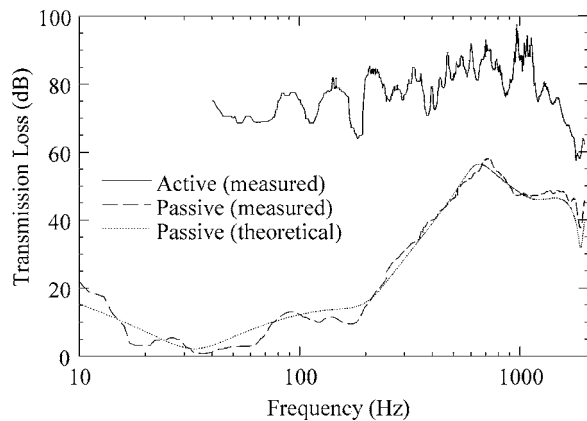
FIG. 10. Measured transmission losses for the DCL ASP module in its passive mode (actuator terminals open circuited) and in its first active mode (transmitting diaphragm acceleration minimized). The measured passive curve is plotted against a theoretical prediction.

FIG. 11. Measured acceleration error signal attenuation produced by a single-channel filtered-*x* controller with the DCL ASP module. The result is plotted against an attenuation curve for the cavity pressure immediately behind the center of the transmitting diaphragm under acceleration control.

though the average transmission loss over the entire measurement bandwidth is 43 dB, it is only 10 dB between 40 and 200 Hz. These low-frequency limitations are typical of passive partitions.

The dip near 200 Hz in the measured curve corresponds approximately to the mass-air-mass resonance frequency of the passive double-leaf partition.[31] Immediately above this dip, the transmission loss increases at slightly more than 20 dB per octave, as anticipated for frequencies just above the resonance. As the frequency continues to increase, one might expect the transmission loss to continue rising at a rate of about 18 dB per octave. However, the trend stops at approximately 720 Hz, at a maximum value of 58 dB. The reduction of the transmission loss above this frequency (following primarily from the presence of the actuator diaphragm surround) suggests a limitation to the idealized double-leaf partition behavior that might be ascribed to the passive module. From 720 to 950 Hz, transmission loss gradually recedes to approximately 47 dB, where it temporarily levels off. Near 1890 Hz, a pronounced dip to a value of 38 dB corresponds to the first axial resonance frequency of the enclosed cavity.

2. Transmitting diaphragm acceleration control

Once the normal acceleration of the transmitting diaphragm was minimized via active control, the transmission loss of the module dramatically increased over the entire measurement bandwidth (see Fig. 10). It increased by an average of 34 dB and by more than 70 dB at some lower frequencies. The transmission loss was not infinite, as predicted by limited theoretical modeling,[17] but it was substantial. Its general value gradually increased from about 70 dB near 40 Hz to over 90 dB near 725 Hz. Above 725 Hz, it decreased until it dropped to roughly 60 dB at the highest measurement frequencies. The average over the entire measurement bandwidth was approximately 77 dB. From 40 to 200 Hz, the average was 73 dB—a 63 dB improvement over the corresponding average under passive conditions. Between 40 and 1125 Hz, the average transmission loss was 82 dB.
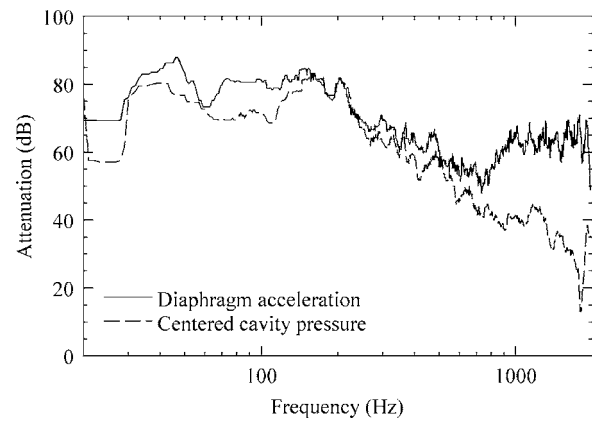
As shown in Fig. 11, the active attenuation of the normal acceleration error signal ranged from a low of about 50 dB at some frequencies to more than 80 dB at several frequencies below 200 Hz. (Such high values for the 12-bit controller I/O system were made possible in part by error signal compression.) The attenuation notably decreased between the lowest frequencies and 750 Hz. Above 750 Hz, it again increased until it leveled off at roughly 64 dB. The average reduction over the entire measurement bandwidth was 64 dB.

The attenuation of the cavity pressure directly behind the center of the transmitting diaphragm is also shown in Fig. 11 as a result of the acceleration control scheme. It clearly follows the acceleration attenuation up to about 750 Hz, but continues its decline at higher frequencies, dropping well below the acceleration attenuation curve. It eventually dips to a conspicuous minimum of 13 dB centered near 1800 Hz. The center frequency of this dip coincides closely with the cutoff frequency of the first cavity cross mode. At frequencies above the dip, the cavity pressure attenuation again rises to approximately 35 dB. On average, cavity pressure attenuation over the measurement bandwidth is 45 dB, a full 19 dB less than the corresponding average acceleration attenuation.

Another noteworthy characteristic of the controlled module involves the normal acceleration at the center of the *actuator* diaphragm. Under controlled conditions, its mean-square value was found to decrease from its passive mean-square value below 800 Hz. However, above 800 Hz, it actually *increased* in order to minimize the normal transmitting diaphragm acceleration. The greatest increase in its mean-square acceleration occurred at approximately 1850 Hz. Theoretical work has indicated that the transmitting diaphragm acceleration control is accomplished by minimizing the source-side volume velocity into the cavity.[2,3,17] Although the rigid body motion of the actuator diaphragm could not be guaranteed over the entire measurement bandwidth, the fact that the relative central diaphragm acceleration increased with increasing frequency suggests that the diaphragm had to counteract at least one other transmission path into the cavity. A principal candidate for such a path was the resilient diaphragm surround.
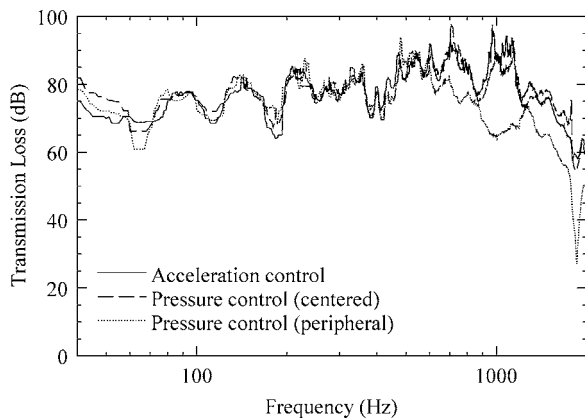
FIG. 12. Measured transmission losses for the DCL ASP module in three active modes: (1) transmitting diaphragm acceleration control, (2) cavity pressure control with the error microphone centered behind the transmitting diaphragm, and (3) cavity pressure control with the error microphone directly behind the transmitting diaphragm surround.

FIG. 13. A comparison of measured transmission losses for the SCL and DCL ASP modules in their passive and acceleration-controlled active modes.

3. Cavity acoustic pressure control

a. Central cavity position   Figure 12 shows that when acoustic pressure was controlled at the central position behind the transmitting diaphragm, the module transmission loss characteristics were very similar to those attained under transmitting diaphragm acceleration control. The average transmission loss over the measurement bandwidth was again 77 dB.

The error signal reduction for this scheme was also similar to that produced by the acceleration control scheme over most of the measurement bandwidth. The average attenuation was again 64 dB. This stands in contrast to the 45 dB average pressure reduction realized under acceleration control at the same cavity position. Over a small bandwidth centered at approximately 180 Hz (near the passive mass-air-mass resonance frequency of the module) there was a significant difference between the error signal attenuation of the two control schemes. Acoustic pressure reduction under cavity pressure control was approximately 12 dB less than acceleration reduction under transmitting diaphragm acceleration control. Acoustic pressure was even reduced more through acceleration control at these frequencies than through cavity pressure control.

As one might anticipate, normal transmitting diaphragm acceleration was substantially reduced under the cavity pressure control scheme because of an attendant decrease in the source-side volume velocity into the cavity. This reduction was nearly identical to the cavity pressure reduction under transmitting diaphragm acceleration control over most of the measurement bandwidth (see Fig. 11). Its average attenuation of 43 dB was about 2 dB lower than the cavity pressure attenuation under acceleration control. The most pronounced difference between the two attenuation curves was again concentrated in the small spectral region centered near the passive mass-air-mass resonance frequency. Relative to cavity pressure reduction under acceleration control, acceleration reduction under cavity pressure control suffered a 13 dB dip in this region. Thus, although the two control schemes demonstrated similar behaviors, the acceleration control scheme was slightly more effective.
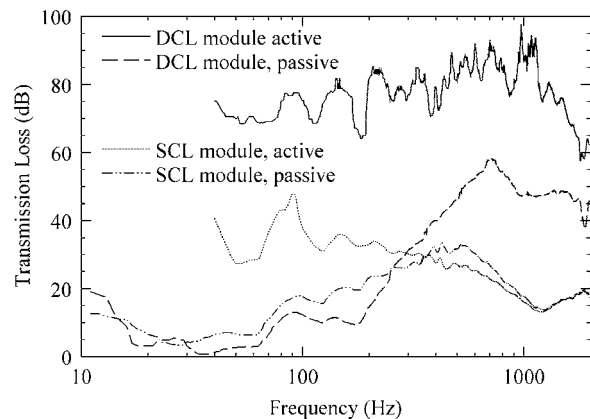
b. Peripheral cavity position   Figure 12 also shows that the controlled transmission loss of the module suffered more significantly after the error microphone was moved from behind the center of the transmitting diaphragm to a peripheral position behind its surround. The transmission loss followed that generated under acceleration control and that generated under centered cavity pressure control up to about 600 Hz. However, above 600 Hz, its relative transmission loss significantly decreased, dropping from roughly 85 dB at 600 Hz to about 50 dB at 1970 Hz. The average value over the entire measurement bandwidth was 68 dB—a full 9 dB lower than that achieved under the other two schemes. The approach also produced a more pronounced dip to 27 dB near 1850 Hz. Interestingly, the transmission loss was even 12 dB lower at that frequency than that produced by the module in its passive state.

Error signal attenuation for this latter scheme once again resembled that of the acceleration control scheme, except near 180 Hz. At that frequency, its relative attenuation dropped by approximately 15 dB. Average attenuation over the measurement bandwidth was 63 dB. The attenuation of normal transmitting diaphragm acceleration was similar to that achieved by the centered cavity pressure control scheme up to about 400 Hz. However, above 400 Hz, it dropped until it became roughly 20 dB less than that achieved by the former scheme over the remaining measurement bandwidth. The attenuation dip centered at 1800 Hz (see Fig. 11) also shifted up slightly to a center frequency of 1850 Hz. The average diaphragm acceleration reduction over the entire measurement bandwidth was 29 dB—a full 14 dB less than that achieved when pressure was minimized at the central cavity position.

IV. DISCUSSION

Figure 13 compares the transmission loss curves for the two ASP modules in their passive and active acceleration-controlled states. While both modules utilized the same basic control objective, the DCL module yielded an average transmission loss improvement of 56 dB over the SCL module.

This significant improvement followed from a simple configurational difference that produced very high transmission loss over a broad frequency range.

Experimental results indicated that both normal transmitting diaphragm acceleration control and centered cavity pressure control of the DCL module yielded similar transmission losses. Both schemes performed best at frequencies well below the cutoff frequency of the first cavity cross mode and the first cavity axial resonance frequency. Assuming the transmitting diaphragm behaved as a translational piston, one would expect diaphragm acceleration control to be less sensitive to error sensor location than cavity pressure control. This assertion is partly supported by the degraded experimental results for cavity pressure control when the error microphone was displaced to the periphery of the cavity. Transmitting diaphragm acceleration control also provided slightly superior error signal reduction than either cavity pressure control scheme.

Many of the results described for the cavity pressure control scheme give evidence of acoustic wave effects increasing in the cavity with increasing frequency. Since these effects make the scheme less consistent at higher frequencies, error microphone placement must be optimized to reduce their impact. Another detrimental aspect of the scheme appears at lower frequencies near the mass-air-mass resonance frequency of the module. As indicated in Ref. 17, cavity pressure control is slightly precarious because it is possible to minimize acoustic pressure at a point in the cavity while the transmitting diaphragm is still vibrating. If an error microphone is positioned near an uncontrolled cavity pressure node, control complications may arise. Because of these limitations of the pressure control scheme, acceleration control might be considered the more effective strategy for the module.

The transmission loss of the SCL module was relatively low at most frequencies. As a result, limitations posed by flanking transmission, electronic cross-talk, and noise were not generally significant during its measurements. With the module rigidly attached to both the source tube and receiving tube, Figs. 7 and 8 suggest that flanking transmission may only have caused a slight effect on the measured transmission loss in a narrow frequency band near 90 Hz.

Because of the very high transmission loss produced by the DCL module, one might question whether the measurement system could accurately evaluate its full transmission loss capabilities. In Sec. II D we indicated that measurement constraints due to flanking transmission, electronic cross-talk, and noise posed significant limitations. To further consider the impact of these limitations, the transmission loss of the acceleration-controlled DCL module is plotted again in Fig. 14, against the transmission loss signal-to-noise ratio[3] and the transmission loss for benchmark partition 4 with its resilient coupler connection. An inspection of the curves reveals that the transmission loss of the DCL module was generally within the transmission loss signal-to-noise ratio, although it pushed these limits at some frequencies. The DCL module also pushed the limits suggested by the benchmark partition up to about 1150 Hz. However, above 1150 Hz, its transmission loss receded, creating a significant margin.
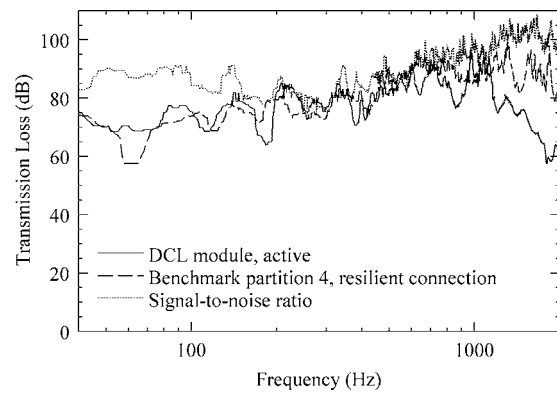

FIG. 14. A comparison of the measured transmission loss of the DCL ASP module under transmitting diaphragm acceleration control to (1) the measured transmission loss of benchmark partition 4 with a resilient coupler connection (see Fig. 5) and (2) the transmission loss signal-to-noise ratio.

Results from Sec. II D suggest that the benchmark partition transmission loss may have been slightly corrupted by flanking transmission below about 160 Hz (see Fig. 7). An inspection of Fig. 14 suggests that the low-frequency portions of the measured ASP module transmission loss may also have been corrupted. However, an additional comparison of Fig. 7 suggests that effects of flanking transmission could have been much worse had the two module sections not been mechanically isolated through their resilient connection.

Transmission loss for the benchmark partition could also have been slightly corrupted by electronic cross-talk between upstream and downstream signals—most predominantly in the spectral region between 500 and 1000 Hz. Once again, this possibility could have implications for the DCL module. Since identical adaptive controller convergences could not be guaranteed for consecutive measurements, upstream and downstream acoustic pressures were measured simultaneously. Otherwise, the effects of electronic cross-talk might have been further reduced.

As shown in Figs. 8 and 10, the measured and theoretically predicted transmission loss curves for the ASP modules have been found to agree within reason. This provides useful validation of the models presented in Ref. 17. Measured and theoretically predicted source-side reflection coefficients of the modules have also been found to agree.[3,17]

V. SUMMARY AND CONCLUSIONS

Experimental methods have been developed to assess the normal-incidence transmission losses of individual active segmented partition (ASP) modules over a bandwidth from 40 to 1970 Hz. The methods fulfill simultaneous dynamic range requirements of a measurement system and an adaptive controller while addressing adaptive controller stability and convergence. Steps were taken to evaluate and reduce flanking transmission, electronic cross-talk, ambient acoustic noise, and electronic noise—all of which limited the maximum reliably measured transmission loss of the system. The module measurements were validated by comparing their

measured transmission losses to theoretical predictions and measured transmission losses of passive benchmark partitions with predictable or extreme behaviors.

Two experimental ASP modules were created to substantiate theoretical predictions of their behaviors. The first was a single-composite-leaf (SCL) configuration with an electromechanically actuated diaphragm and a resilient surround. The second was a double-composite-leaf (DCL) configuration with an electroacoustically actuated cavity bounded by a passive transmitting diaphragm and a resilient surround. The underlying active control objective for each was to induce global reduction of its normal transmitting surface vibrations through simple actuation and error sensing.

A filtered-x adaptive controller successfully controlled both modules over the entire measurement bandwidth as they were excited by a swept-sinusoidal stimulus. Electronic signal compression was found to increase error signal attenuations, sometimes to exceptional values for the 12-bit controller I/O system. Nevertheless, actual transmission loss performances of the modules depended more significantly upon their physical configurations and control schemes.

Under active transmitting diaphragm acceleration control, the low-frequency transmission loss of the SCL module increased somewhat over its passive transmission loss, but the high-frequency transmission loss decreased, leaving the average value unchanged. The decline in high-frequency performance was apparently caused by uncontrolled surround vibrations. Under similar control, the transmission loss of the DCL module increased substantially at all frequencies. Increases at low frequencies were particularly noteworthy. Flanking transmission, electronic cross-talk, and noise may have had some influence on the measurement of its very high transmission loss values.

The adaptive controller was also used in an alternative control scheme to minimize acoustic pressure at discrete points within the DCL module cavity. Transmitting diaphragm acceleration control was found to be slightly more effective than cavity pressure control when the error microphone was centered directly behind the transmitting diaphragm. It was found to be much more effective than cavity pressure control when the microphone was moved to the periphery of the cavity. Inefficiencies of the cavity pressure control scheme stem from acoustic wave effects in the cavity at higher frequencies and other problems related to error signal observability. Transmitting diaphragm acceleration control and cavity pressure control both performed best at frequencies well below the cutoff frequency of the first cavity cross mode and the frequency of the first axial cavity resonance.

Under active control, the mean-square acceleration at the center of the DCL module actuator diaphragm actually increased from its passive value at higher frequencies. This increase was apparently required to counteract one or more transmission paths into the module cavity (other than the central part of the diaphragm itself) and to reduce the source-side volume velocity. The actuator surround was a likely candidate for an alternative path into the cavity.

While both modules used the same underlying control objective, the DCL module yielded an average transmission loss that was 56 dB higher than that of the SCL module. This substantial improvement was accomplished through a simple configurational change that required no more complicated actuation or error sensing. While both modules improved low-frequency transmission loss through active control, the DCL module consistently provided much higher transmission loss over the entire measurement bandwidth. It therefore proved to be the better candidate for ASP applications.

Additional work is required to assess normal-incidence transmission loss characteristics of other ASP module configurations and multiple modules mounted in ASP arrays. Oblique and random-incidence transmission loss measurements should also be conducted for these modules and arrays.

ACKNOWLEDGMENTS

[1] T. W. Leishman, "Research in the field of active sound transmission control," J. Acoust. Soc. Am. **114**, 2390(A) (2003).

[2] T. W. Leishman and J. Tichy, "A fundamental investigation of the active control of sound transmission through segmented partition elements," Proceedings of Noise-Con 97, University Park, Pennsylvania, USA, 1997, Vol. 2, pp. 137–148.

[3] T. W. Leishman, "Active control of sound transmission through partitions composed of discretely controlled modules," Ph.D. thesis, The Pennsylvania State University, University Park, Pennsylvania, 2000.

[4] D. R. Thomas, P. A. Nelson, and S. J. Elliott, "An experimental investigation into the active control of sound transmission through stifflight composite panels," Noise Control Eng. J. **41**, 273–279 (1993).

[5] D. R. Thomas, P. A. Nelson, R. J. Pinnington, and S. J. Elliott, "An analytical investigation of the active control of the transmission of sound through plates," J. Sound Vib. **181**, 515–539 (1995).

[6] S. L. Sharp, G. H. Koopmann, and W. Chen, "Transmission loss characteristics of an active trim panel," Proceedings of Noise-Con 97, University Park, Pennsylvania, 1997, Vol. 2, pp. 149–160.

[7] R. L. St. Pierre, Jr., G. H. Koopmann, and W. Chen, "Volume velocity control of sound transmission through composite panels," J. Sound Vib. **210**, 441–460 (1998).

[8] S. M. Hirsch, J. Q. Sun, and M. R. Jolly, "An analytical study of interior noise control using segmented panels," J. Sound Vib. **231**, 1007–1021 (2000).

[9] S. M. Hirsch, N. E. Meyer, M. A. Westervelt, P. King, F. J. Li, M. V. Petrova, and J. Q. Sun, "Experimental study of smart segmented trim panels for aircraft interior noise," J. Sound Vib. **231**, 1023–1027 (2000).

[10] G. P. Mathur, C. L. Chin, M. A. Simpson, and J. T. Lee, "Structural acoustic prediction and interior noise control technology," NASA/CR-2001-211247, 2001.

[11] J. E. Cole, III and M. C. Junger, "Active noise control for machinery enclosures," NSF Final Report U-1944-379F, 1991.

[12] J. E. Cole, K. F. Martini, and A. W. Stokes, "Active noise control for machinery enclosures," NSF Final Report U-2413-393, 1996.

[13] R. S. Jackson, "The performance of acoustic hoods at low frequencies," Acustica **12**, 139–152 (1962).

[14] T. W. Leishman and J. Tichy, "An experimental evaluation of individual partition segment configurations for the active control of sound transmission," J. Acoust. Soc. Am. **104**, 1776(A) (1998).

[15] T. W. Leishman and J. Tichy, "An experimental investigation of a novel active segmented partition for sound transmission control," J. Acoust. Soc. Am. **105**, 1156(A) (1999).

[16] T. W. Leishman, "Vibration-controlled modules for use in active segmented partitions," J. Acoust. Soc. Am. **114**, 2385(A) (2003).

[17]T. W. Leishman and J. Tichy, "A theoretical and numerical analysis of vibration-controlled modules for use in active segmented partitions," J. Acoust. Soc. Am. **118**, 1424-1438 (2005).

[18]One easily overlooked complication in the measurement of active partitions involves the impact of actuation upon both the receiving space and source space sound fields. When comparing passive and active control conditions for a partition, a change to either field has impact on the measured transmission loss. Another complication involves the interaction between active partitions, as secondary sources of sound, and primary sources of sound in the source space (Ref. 19). Other complications are discussed in this paper.

[19]T. W. Leishman and J. Tichy, "On the significance of reflection coefficients produced by active surfaces bounding one-dimensional sound fields," J. Acoust. Soc. Am. **113**, 1475–1482 (2003).

[20]J. Y. Chung and D. A. Blaser, "Transfer function method of measuring in-duct acoustic properties. I. Theory," J. Acoust. Soc. Am. **68**, 907–913 (1980).

[21]J. Y. Chung and D. A. Blaser, "Transfer function method of measuring in-duct acoustic properties. II. Experiment," J. Acoust. Soc. Am. **68**, 914–921 (1980).

[22]B. E. Anderson and T. W. Leishman, "An acoustical measurement method for the derivation of loudspeaker parameters," AES 115th Convention, New York, NY, USA, 2003, preprint 5865, pp. 1–13.

[23]Although ASP modules are typically rectangular in cross section, circular tube and module geometries are investigated in this work with no loss of generality for the evaluation of individual modules.

[24]L. L. Beranek and H. P. Sleeper, Jr., "The design and construction of anechoic sound chambers," J. Acoust. Soc. Am. **18**, 140–150 (1946).

[25]"Standard test method for impedance and absorption of acoustical materials by the impedance tube method," American Society for Testing and Materials, ASTM Designation: C384–88 (1988).

[26]"Standard test method for impedance and absorption of acoustical materials using a tube, two microphones, and a digital frequency analysis system," American Society for Testing and Materials, ASTM Designation: E1050–90 (1990).

[27]H. Bodén and M. Åbom, "Influence of errors on the two-microphone method for measuring acoustic properties in ducts," J. Acoust. Soc. Am. **79**, 541–549 (1986).

[28]J. D'Appolito, *Testing Loudspeakers* (Audio Amateur Press, Peterborough, NH, 1998).

[29]Arithmetic decibel averages are used in this paper. Because they are based on fixed 1 Hz frequency increments, these averages are most easily visualized with transmission loss plots that use linear frequency scales.

[30]When used for error signal processing, the compressor/limiter was adjusted to send the adaptive controller consistently high error signal levels throughout the adaptation processes. With sinusoidal excitation and a compression ratio of approximately 8:1, it allowed adaptation to proceed without significant effect on convergence or stability. It also enabled the adaptive controller to significantly improve its error signal reductions (Ref. 3).

[31]F. J. Fahy, *Sound and Structural Vibration: Radiation, Transmission, and Response* (Academic Press, New York, 1985).

[32]Without the use of the compressor/limiter, the average acceleration reduction over the measurement bandwidth was approximately 63 dB. With its use, the value increased to approximately 66 dB—a 3 dB improvement. However, between 20 and 100 Hz, the compressor/limiter produced an average improvement of 10 dB, while between 200 and 600 Hz it produced an average improvement of 9 dB. Over the remainder of the bandwidth, the compressed and uncompressed error signals yielded similar reductions, with a few exceptions. Error signal compression might be considered for the enhancement of adaptive controllers with inadequate dynamic ranges, at least when used with sinusoidal stimuli.